Measurement of cosmic-ray muon flux at CJPL-II

P. Zhang^a, H. Ma^a, W. Dai^a, M. Jing^a, L. Yang^a, Q. Yue^a, Z. Zeng^{a,*} and J. Cheng^{a,b,**}

ARTICLE INFO

Keywords: CJPL-II Cosmic-ray muon flux Plastic scintillator Detection efficiency

ABSTRACT

In China Jinping Underground Laboratory (CJPL), the deepest and largest underground laboratory globally, the cosmic-ray muon flux is significantly reduced due to the substantial shielding provided by the overlying mountain. From 2016 to 2020, we measured the muon flux in the second phase of CJPL (CJPL-II) with a plastic scintillator muon telescope system, detecting 161 muon events over an effective live time of 1098 days. The detection efficiency was obtained by simulating the underground muon energy and angular distributions and the telescope system's response to underground muons. The cosmic-ray muon flux is determined to be $(3.03 \pm 0.24 \, (\text{stat}) \pm 0.18 \, (\text{sys})) \times 10^{-10} \, \text{cm}^{-2} \text{s}^{-1}$, which is the lowest among underground laboratories worldwide.

1. Introduction

China Jinping Underground Laboratory (CJPL), located within the 17.5 km long traffic tunnel of the Jinping Mountain in Sichuan Province, China, is shielded by approximately 2,400 m of vertical rock coverage [1, 2]. This extensive rock shielding significantly reduces the cosmic-ray muon flux, thereby minimizing the muon and muon-induced radiation backgrounds [3–5] and making CJPL an ideal site for rare-event experiments, such as direct dark matter detection and neutrinoless double- β decay experiments [2].

The first phase of the laboratory (CJPL-I) began construction in 2009 and officially became operational in 2010, with a total space of approximately $4,000\,\mathrm{m}^3$ [2]. In 2013, using a plastic scintillator muon telescope system, the cosmic-ray muon flux at CJPL-I was measured to be $(2.0 \pm 0.4) \times 10^{-10} \,\mathrm{cm}^{-2}\mathrm{s}^{-1}$, without efficiency correction to the detector angular acceptance [1]. In 2021, the efficiency-corrected cosmic-ray muon flux at CJPL-I was determined to be $(3.53 \pm 0.23) \times 10^{-10} \,\mathrm{cm}^{-2}\mathrm{s}^{-1}$ based on data from a liquid scintillator prototype system for solar neutrino detection [5].

The second phase (CJPL-II), located about 500 m west of CJPL-I along the same traffic tunnel, finished the civil engineering and decoration in 2024 with a capacity of 300,000 m³ [2]. This study employed the same plastic scintillator muon telescope system[1] to measure the cosmic-ray muon flux in the hall C2 of CJPL-II.

This article is structured as follows: Section 2 details the experiment, the simulation of the underground muon distributions and the telescope system's response to underground muons. Section 3 presents the results of the experiment and simulation. Conclusions are drawn in Section 4.

2. Experiment and methods

From October 2016 to December 2020, we conducted a measurement of the cosmic-ray muon flux in the hall C2 of CJPL-II using a plastic scintillator muon telescope system. The telescope system, depicted in Figure 1, comprises two groups of plastic scintillators, each containing three detectors. The size of each detector is 1 m \times 0.5 m \times 0.05 m. The distances between neighboring detectors (vertically/horizontally) are both about 0.2 m [1]. With ultrahigh energy and strong penetration capability, a cosmic-ray muon could pass through all three detectors in a group, resulting in triple coincidence signals with large amplitudes. The muon candidates were selected after the data quality check (remove data batches with abnormal trigger rate), the rise/fall time restrain and the amplitude restrain [1]. For simplification, we didn't apply anti-coincidence between two groups in the event selection. Figure 2 shows the detector waveforms of a muon candidate. The measured muon flux $\phi_{\rm m}$ (efficiency-uncorrected) is calculated as follows:

$$\phi_{\rm m} = \frac{N_{\mu}}{S_{\rm d} \cdot T} \tag{1}$$

where N_{μ} is the number of the selected muon candidates, $S_{\rm d}$ (0.5 m²) is the upper surface area of the detector, and T is the experimental live time.

On the one hand, only part of the muons passing through the top detectors could be selected as the muon candidates. On the other hand, the selected muon candidates may be contaminated by high-energy muon shower events, which are generated when muons pass through rock around the laboratory. Therefore, the actual integrated muon flux ϕ (efficiency-corrected) is related to the measured muon flux $\phi_{\rm m}$ with the overall detection efficiency ϵ :

$$\phi = \frac{\phi_{\rm m}}{\epsilon} \tag{2}$$

To calculate the detection efficiency, we firstly need to determine the energy and angular distributions of

^aKey Laboratory of Particle and Radiation Imaging (Ministry of Education) and Department of Engineering Physics, Tsinghua University, Beijing 100084, China

^bSchool of Physics and Astronomy, Beijing Normal University, Beijing 100875, China

^{*}Corresponding author: zengzhi@tsinghua.edu.cn

^{**}Corresponding author: chengjp@tsinghua.edu.cn ORCID(s): 0000-0003-1243-7675 (Z. Zeng)

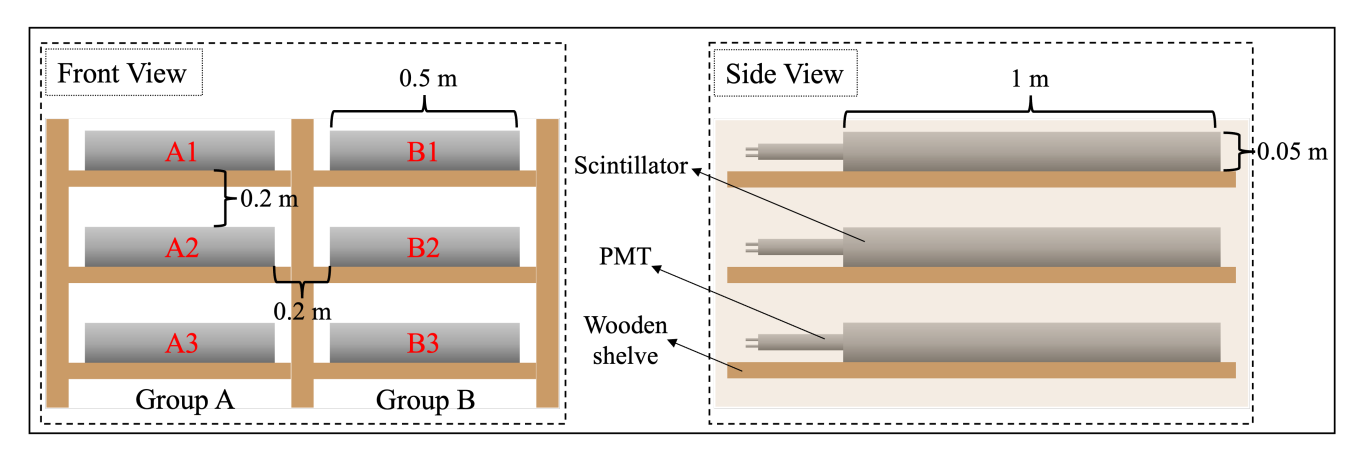


Figure 1: Schematic of the muon telescope system

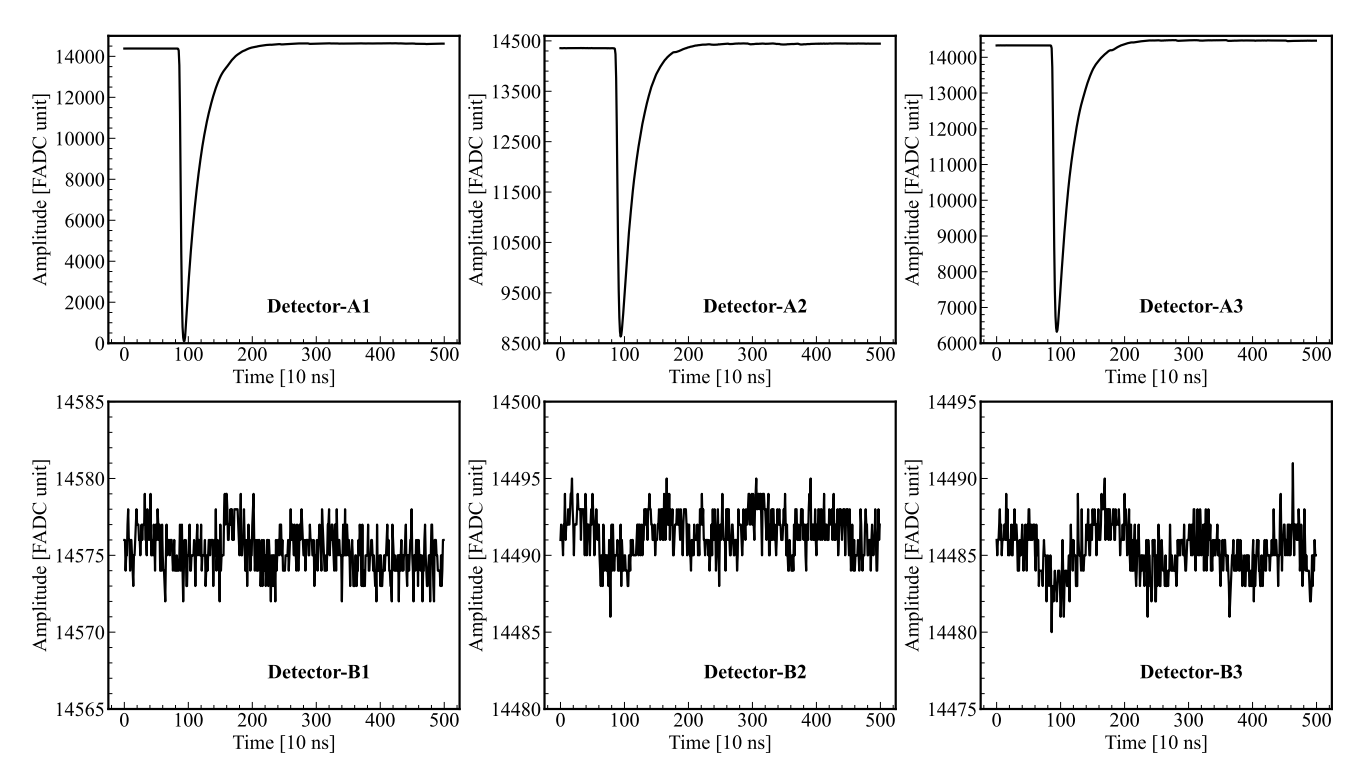


Figure 2: Detector waveforms when a muon passed all three detectors of group A. The deposited energy in the A1, A2 and A3 detectors are 19.3, 9.7 and 12.3 MeV.

underground muons by simulating the transportation of high-energy muons through the mountain above. Then, the detection efficiency is calculated by simulating the telescope system's response to underground muons.

CJPL is located beneath the Jinping Mountain, at an altitude of approximately 1,600 m, with a rock overburden of about 2,400 m. The Google Earth program[6] was utilized to obtain the latitude, longitude, and elevation of 18,529 points on the mountain surface within an 8 km radius circle centered at the CJPL-II, with a grid size of 0.001 degree × 0.001 degree (latitude × longitude). The geometry model of the Jinping Mountain is visualized in Figure 3. We employed a modified Gaisser Formula to sample the incident high-energy muons [7]. The angular

dependence of muon energy distribution is considered. For each muon, the depth of rock along the muon's path to the laboratory was calculated. Then, we simulated the transportation of each muon using the MUSIC program [8], which was widely used in the muon flux simulations for underground laboratories. The average density and the composition of rock follow the setting in Ref. [5]. The muon energy and angular distributions underground were obtained by analyzing the transportation results.

We utilized the Geant4 program [9–11] to simulate the telescope's response to underground muons. As illustrated in Figure 4, we constructed a geometry model in Geant4 with the internal size of the experimental hall set to 129 m \times 14 m \times 14 m. We added 1 m thick rock around the hall

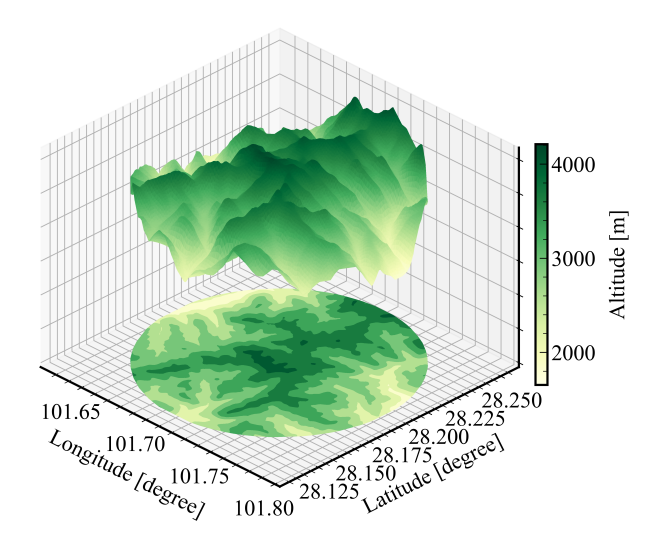


Figure 3: Geometry model of the Jinping Mountain

to simulate the electromagnetic shower initiated by muon, following the setting in Ref. [5]. Upon evaluation, 1 m thick rock is thick enough and the result variation is within the margin of error when the depth is set bigger. The density and composition of rock were set the same with those used in the muon transportation simulation. With the simulated underground muon distributions, muon events were sampled on a sampling plane above the experimental hall. The sampling plane was set big enough so that the muons that could pass through the experimental hall could be sampled from the sampling plane.

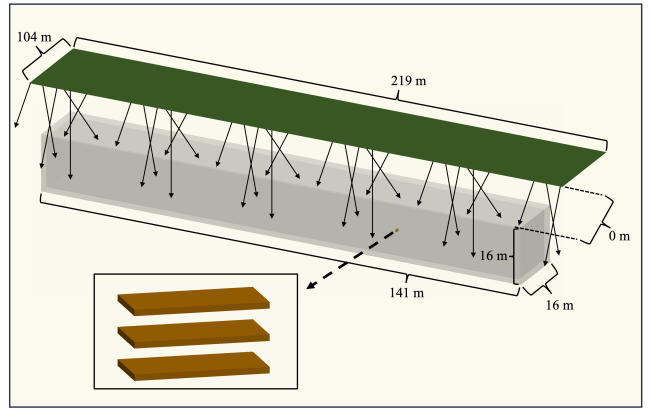


Figure 4: Visualization of the telescope system (zoomed in) at the hall C2 of CJPL-II. The green plane represents the sampling plane, which is in the same plane of the upper surface of the rock layer

. The arrows illustrated the tracks of the sampled underground muons.

Let N denote the total number of the muons simulated, $N_{\rm a}$ the number of the muons passing through all three detectors, and $N_{\rm t}$ the total number of events passing the energy threshold. Thus, the angular acceptance $\epsilon_{\rm a}$ and the

overal efficiency ϵ are calculated as follows:

$$\epsilon_{\rm a} = \frac{N_{\rm a} \cdot C_r}{N}, \epsilon = \frac{N_{\rm t} \cdot C_r}{N}$$
 (3)

$$C_r = \frac{S_s}{S_d} \tag{4}$$

where S_s (22750 m²) is the area of the sampling plane. With the factor C_r introduced, the top detector upper surface plane becomes the reference plane of the efficiencies. The angular acceptance ϵ_a is equivalent to the so called "solid angle correction factor", which is defined as the ratio of the number of the muons passing through all three detectors over the number of the muons passing through the top detector [1].

3. Cosmic-ray muon flux at CJPL-II

After the data quality check, 8.5 days of data were discarded, and then we obtained a dataset with an effective live time of 1098 days. The energy calibration was performed by comparing the simulated energy distribution and the measured amplitude distribution. The systematic uncertainty of the obtained energy is about 3.1%. The energy threshold for event selection was set to 7.3 MeV, which is the lower energy limit of the muon spectrum peak. Figure 5 presents the energy spectra of triple coincidence signals. The measurement results are summarized in Table 1. Among total 161 events, there are 85 events from group A and 76 events from group B. Besides, there are four pairs of coincidental events between group A and group B, which corresponds to the expectation from simulation.

Combining the data from two groups, the measured muon flux $\phi_{\rm m}$ was determined to be $(1.70\pm0.13)\times10^{-10}$ cm⁻²s⁻¹, while the same telescope system yielded a result of $(2.0\pm0.4)\times10^{-10}$ cm⁻²s⁻¹ at CJPL-I in 2013 [1]. As shown in Figure 6, we grouped the data into four-month intervals and calculated the flux for each interval. In the shallower underground laboratories, seasonal modulations of the muon flux were observed [12, 13]. In this study, no modulation effect of the muon flux over time was observed (In the flat distribution assumption, $\chi^2/\text{d.o.f} = 19.3/16$, p-value = 0.25), due to significant statistical fluctuations.

To calculate the energy and angular distributions of underground muons, a total of 2×10^7 high-energy incident muons were simulated. The distribution of depth of rock that the incident muons traverse is shown in polar coordinates in Figure 7. The angular distribution of the underground muons is shown in Figure 8. Simulation results indicates that the angular distribution of the surviving muons is consistent with the distribution of the depth of rock that the incident muons traverse. A significant portion of the muon flux at CJPL-II originates from the northwest and southwest, with zenith angles of 20-40 degrees, where the rock layer is thinner. The energy and angular distributions of muons on the ground and underground are compared in Figure 9. The mountain reduces the flux of 4 GeV muons by approximately 9 orders of magnitude and the integral flux by about 8 orders of magnitude. The average energy of the underground

Table 1
Results of cosmic-ray muon flux measurement

Detector group	Live time (days)	Number of muon events	Muon flux $(cm^{-2}s^{-1})$
A	1098	85	$(1.80 \pm 0.19) \times 10^{-10}$
В	1098	76	$(1.60 \pm 0.18) \times 10^{-10}$
Total	1098	161	$(1.70 \pm 0.13) \times 10^{-10}$

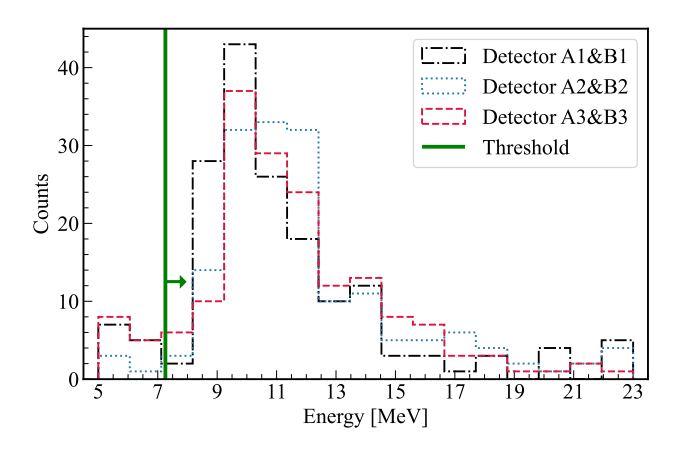


Figure 5: Energy spectra of triple coincidence signals

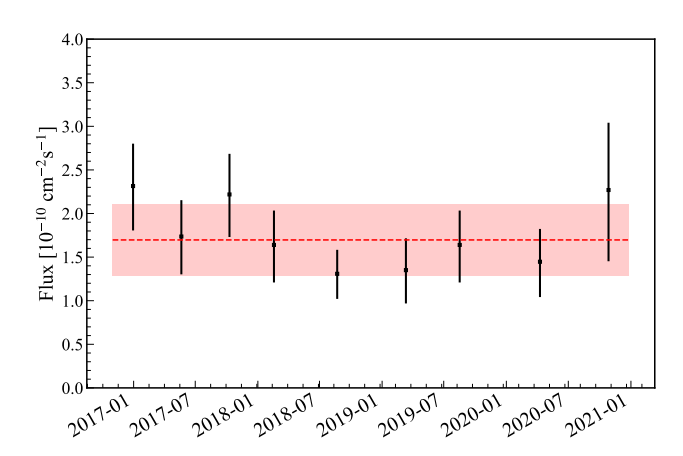


Figure 6: Measured cosmic-ray muon flux over time without efficiency correction

muons is 359.6 GeV, which is close to the results in Ref. [4, 5].

With the simulated underground muon distributions, we sampled 1×10^9 underground muons to simulate the response of the telescope system. The muons with zenith angle above 70 degrees are ignored in the simulation because they contribute less than 0.04% of the detector counts. The angular acceptance e_a and the overall efficiency e were determined to be 0.510 ± 0.005 (stat) ±0.046 (sys) and 0.562 ± 0.005 (stat) ±0.033 (sys). The angular acceptance is bigger than the value of 0.339 on the ground [1], because the angular distribution of the muons at CJPL-II is more vertical than that on the ground, as shown in Figure. 9.

The uncertainty sources of the overall efficiency are

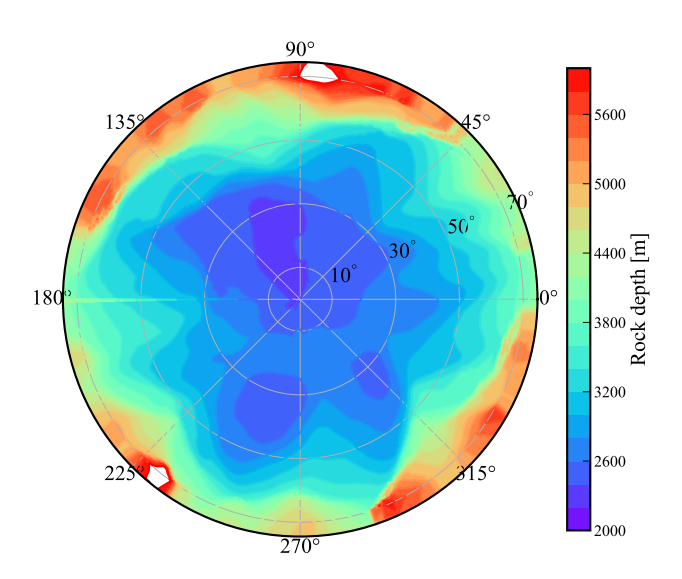


Figure 7: Distribution of depth of rock that the incident muons traverse. The radial coordinate represents the zenith angle, and the angular coordinate represents the azimuth angle (degree 0 corresponds to the east direction).

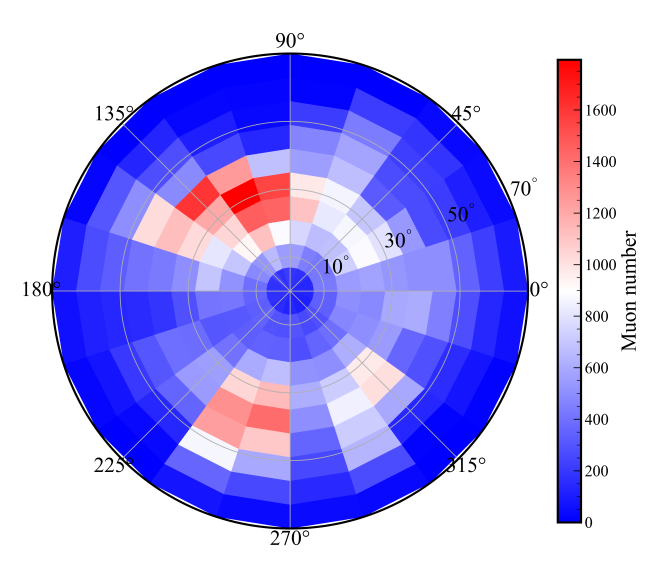


Figure 8: Simulated angular distribution of the underground muons in polar coordinates The radial coordinate represents the zenith angle, and the angular coordinate represents the azimuth angle (degree 0 corresponds to the east direction).

summarized in Table 2. The systematic uncertainty of the efficiency arises from three sources: the mountain geometry model, the density of rock and the thickness of rock around

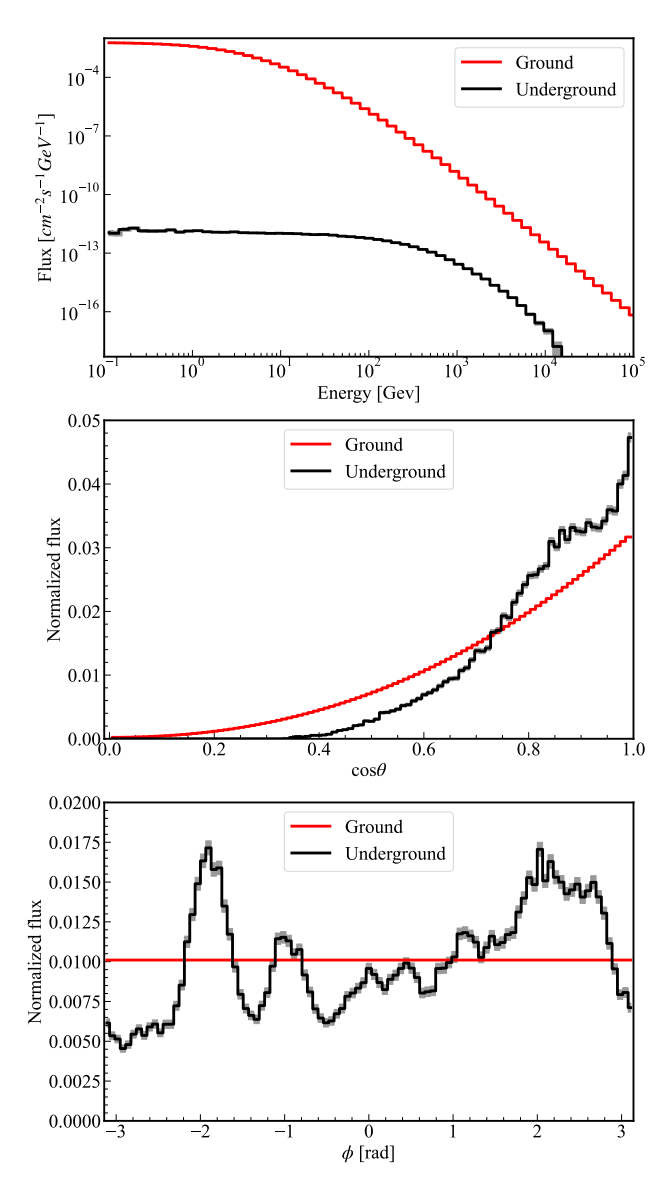


Figure 9: Energy and angular distributions of muons on the ground and underground.

the experimental hall. We evaluated the uncertainty from the mountain geometry model by shifting it by \pm 100 m in the north-south, east-west, and up-down directions, taking the maximum deviation as a part of systematic uncertainty. The uncertainty from the rock density was evaluated by considering variations of \pm 0.1 g/cm³, while the uncertainty from the rock thickness was assessed by considering variations of \pm 0.5 m.

With the measured muon flux $\phi_{\rm m}$ and the overall efficiency ϵ calculated above, we derived that the muon flux ϕ at CJPL-II is $(3.03 \pm 0.24 \ ({\rm stat}) \pm 0.18 \ ({\rm sys})) \times 10^{-10} \ {\rm cm}^{-2}{\rm s}^{-1}$. It is slightly lower than those of SNOLab [14] and CJPL-I [5].

 Table 2

 Summary of uncertainties of the overall efficiency

Uncertainty source	Uncertainty
Systematic (Mountain geometry)	0.019
Systematic (Rock density)	0.022
Systematic (Rock thickness)	0.016
Statistical	0.005
Total	0.033

4. Conclusion

We present a study of the cosmic-ray muon flux measurement using a plastic scintillator muon telescope system at CJPL-II. To calculate the detection efficiency, we first simulated the transportation of muons through the Jinping mountain and obtained the energy and angular distributions of the underground muons. Results indicate that a significant contribution to the muon flux at CJPL-II originates from the northwest and southwest, with zenith angle of 20-40 degrees. Then, using the simulated underground muon distributions, we simulated the telescope system's response to underground muons and derived the detection efficiency. Finally, the cosmic-ray muon flux at CJPL-II was determined to be $(3.03 \pm 0.24 \text{ (stat)} \pm 0.18 \text{ (sys)}) \times 10^{-10} \text{ cm}^{-2}\text{s}^{-1}$, which is the lowest among underground laboratories world-wide.

Acknowledgments

This work was supported by the National Natural Science Foundation of China (Grant No. 12425507 and No. 12175112) and the National Key Research and Development Program of China (Grant No. 2023YFA1607101 and No. 2022YFA1604701). The authors would like to thank Dr. Weihe Zeng for helpful discussion on the MUSIC simulation.

References

- [1] Y. Wu, X. Hao, Q. Yue, Y. Li, J. Cheng, K. Kang et al., Measurement of cosmic ray flux in the China JinPing underground laboratory, Chinese Physics C 37 (2013) 086001.
- [2] J. Cheng, K. Kang, J. Li, J. Li, Y. Li, Q. Yue et al., The China Jinping Underground Laboratory and Its Early Science, Annual Review of Nuclear and Particle Science 67 (2017) 231.
- [3] Z. Zeng, Y. Mi, M. Zeng, H. Ma, Q. Yue, J. Cheng et al., Characterization of a broad-energy germanium detector for its use in CJPL, Nuclear Science and Techniques 28 (2017) 7.
- [4] W. Zeng, H. Ma, M. Zeng, Z. Zeng, Q. Yue, J. Cheng et al., Evaluation of cosmogenic activation of copper and germanium during production in Jinping Underground Laboratory, Nuclear Science and Techniques 31 (2020) 50.
- [5] Z. Guo, L. Bathe-Peters, S. Chen, M. Chouaki, W. Dou, L. Guo et al., Muon flux measurement at China Jinping Underground Laboratory *, Chinese Physics C 45 (2021) 025001.
- [6] Google Inc, "Google Earth." Retrieved 08/12/2011 from https://earth.google.com/.
- [7] M. Guan, M. Chu, J. Cao, K. Luk and C. Yang, "A parametrization of the cosmic-ray muon flux at sea-level." http://arxiv.org/abs/1509.06176, 2015.

- [8] V. Kudryavtsev, Muon simulation codes MUSIC and MUSUN for underground physics, Computer Physics Communications 180 (2009) 339.
- [9] J. Allison, K. Amako, J. Apostolakis, H. Araujo, P. Arce Dubois, M. Asai et al., Geant4 developments and applications, IEEE Transactions on Nuclear Science 53 (2006) 270.
- [10] J. Allison, K. Amako, J. Apostolakis, P. Arce, M. Asai, T. Aso et al., Recent developments in Geant4, Nuclear Instruments and Methods in Physics Research Section A: Accelerators, Spectrometers, Detectors and Associated Equipment 835 (2016) 186.
- [11] S. Agostinelli, J. Allison, K. Amako, J. Apostolakis, H. Araujo, P. Arce et al., Geant4—a simulation toolkit, Nuclear Instruments and Methods in Physics Research Section A: Accelerators, Spectrometers, Detectors and Associated Equipment 506 (2003) 250.
- [12] M. Agostini, K. Altenmüller, S. Appel, V. Atroshchenko, Z. Bagdasarian, D. Basilico et al., Modulations of the cosmic muon signal in ten years of Borexino data, Journal of Cosmology and Astroparticle Physics 2019 (2019) 046.
- [13] H. Prihtiadi, G. Adhikari, E. B. d. Souza, N. Carlin, J. J. Choi, S. Choi et al., Measurement of the cosmic muon annual and diurnal flux variation with the COSINE-100 detector, Journal of Cosmology and Astroparticle Physics 2021 (2021) 013.
- [14] B. Aharmim, S. N. Ahmed, T. C. Andersen, A. E. Anthony, N. Barros, E. W. Beier et al., Measurement of the cosmic ray and neutrino-induced muon flux at the Sudbury neutrino observatory, Physical Review D 80 (2009) 012001.